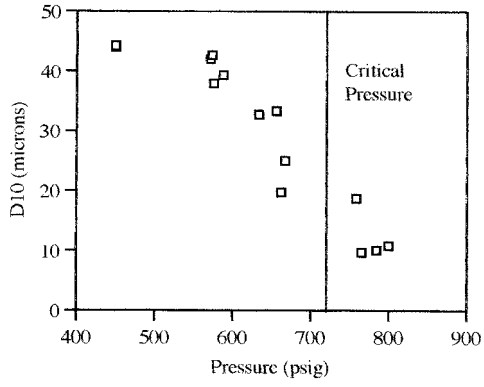

Fig. 2 Arithmetic mean diameter as a function of chamber pressure showing decrease of droplet size with increasing pressure and existence of droplets past the critical pressure of pure oxygen (P_c = 720 psig).

rate dropped with increasing pressure, starting from 26% at 450 psig and going down to 9% at 800 psig. However, the trend was not consistent and the lowest validation rates were not necessarily obtained at the highest chamber pressures, indicating the criticality of a correct optical alignment of the PDPA and a clear optical path through the combustion chamber. Validation rates dropped dramatically when the chamber windows became smudged, cracked, or fogged. These constitute the first ever PDPA droplet measurements for LOX above its critical pressure and temperature, indicating the existence of drops at least slightly above its critical pressure in the pure state, perhaps because of an increase of the critical pressure of oxygen caused by dissolved water vapor or hydrogen.[10] Suspended fuel droplets have been observed experimentally to exist above a fuel's critical pressure and temperature.[11,12]

Conclusions

Experiments were performed with LOX and gaseous hydrogen at elevated pressures with an SSME unielement shear coaxial injector in a subscale rocket combustion chamber. An Aerometrics PDPA was employed to examine the effect of chamber pressure on the LOX droplet size and velocity in the far-field region of the combusting spray. The injector velocity and mixture ratios were held constant and the spray was sampled 12 cm downstream from the injector face and 4 mm off-axis. The droplet arithmetic mean diameter decreased with increasing chamber pressure, whereas no effect on the droplet velocity was measured. For the first time droplet measurements were obtained for chamber pressures 80 psi above the critical pressure of pure oxygen (720 psig), indicating that solubility of hydrogen or water vapor in the oxygen may have increased its critical pressure.

Acknowledgments

This work was supported by the U.S. Air Force Office of Scientific Research Grant F49620-95-1-0184 and NASA Grants NAGW-1356, Supplement 10, and NGT-10034. J.-L. Thomas wishes to acknowledge the financial support of the Societe Europeene de Propulsion. The authors thank the U.S. Army Research Laboratory, Aberdeen, Maryland, for the loan of the Aerometrics PDPA.

References

[1]Bachalo, W. D., and Houser, M. J., "Phase/Doppler Spray Analyzer for Simultaneous Measurements of Drop Size and Velocity Distributions," *Optical Engineering*, Vol. 23, No. 5, 1984, pp. 583–590.

[2]Pal, S., Moser, M. D., Ryan, H. M., Foust, M. J., and Santoro, R. J., "Shear Coaxial Injector Atomization Phenomena for Combusting and Non-combusting Conditions," *Atomization and Sprays*, Vol. 6, No. 2, 1996, pp. 227–244.

[3]Ferraro, M., Kujala, R. J., Thomas, J.-L., Glogowski, M. J., and Micci, M. M., "Effects of GH_2/LOX Velocity and Momentum Ratios on Shear Coaxial Injector Atomization," *Journal of Propulsion and Power* (submitted for publication).

[4]Sankar, S. V., Inenaga, A. S., and Bachalo, W. D., "Trajectory Dependent Scattering in Phase Doppler Interferometry: Minimizing and Eliminating Sizing Errors," 6th Int. Symposium on the Application of Laser Techniques to Fluid Mechanics, July 1992.

[5]Alexander, D. R., Wiles, K. J., Schaub, S. A., and Seeman, M. P., "Effects of Non-Spherical Drops on Phase Doppler Spray Analyzer," *Particle Sizing and Spray Analysis*, Vol. 573, Society of Photo-Optical Instrumentation Engineers, Bellingham, WA, 1985, pp. 67–72.

[6]Bachalo, W. D., Rudoff, R. C., and Brena de la Rosa, A., "Mass Flux Measurements of a High Number Density Spray System Using the Phase Doppler Particle Analyzer," AIAA Paper 88-0236, Jan. 1988.

[7]Pitcher, G., Wigley, G., and Saffman, M., "Sensitivity of Drop-size Measurements by Phase Doppler Anemometry to Refractive Index Changes in Combusting Fuel Sprays," *5th International Symposium on the Applications of Laser Techniques to Fluid Mechanics*, Springer–Verlag, Berlin, 1990, pp. 227–247.

[8]Schneider, M., and Hirleman, E. D., "Influence of Internal Refractive Index Gradients on Size Measurements of Spherically Symmetric Particles by Phase Doppler Anemometry," *Applied Optics*, Vol. 33, No. 12, 1994, pp. 2379–2388.

[9]Bachalo, W. D., and Sankar, S. B., "Factors Affecting the Measurement Resolution and Accuracy of the Phase Doppler Particle Analyzer," 2nd Int. Conf. on Fluid Dynamics Measurements and Its Applications, Tsinghua Univ., Beijing, PRC, Oct., 1994.

[10]Delplanque, J.-P., and Sirignano, W. A., "Numerical Study of the Transient Vaporization of an Oxygen Droplet at Sub- and Super-Critical Conditions," *International Journal of Heat and Mass Transfer*, Vol. 36, No. 2, 1993, pp. 303–314.

[11]Vieille, B., Chauveau, C., Chesneau, X., Odeide, A., and Gokalp, I., "High-Pressure Droplet Burning Experiments in Microgravity," *26th Symposium (International) on Combustion*, The Combustion Inst., Pittsburgh, PA, 1996, pp. 1259–1265.

[12]Nomura, H., Ujiie, Y., Rath, H. J., Sato, J., and Kono, M., "Experimental Study on High-Pressure Droplet Evaporation Using Microgravity Conditions," *26th Symposium (International) on Combustion*, The Combustion Inst., Pittsburgh, PA, 1996, pp. 1267–1273.

General Numerical Model for Liquid Jet Atomization Applications

Yen-Sen Chen* and Huan-Min Shang†
Engineering Sciences, Inc., Huntsville, Alabama 35802
Chien-Pin Chen‡
University of Alabama in Huntsville, Huntsville, Alabama 35899
and
Ten-See Wang§
NASA Marshall Space Flight Center, Huntsville, Alabama 35812

Introduction

NUMERICAL modeling of atomization processes in many liquid-fueled propulsion systems poses a challenge because it requires simultaneous resolution of liquid-gas-droplets dynamics, and the flow regimes considered can range from

Received July 26, 1996; revision received Dec. 2, 1997; accepted for publication March 2, 1998.

*President. Member AIAA.
†Senior Research Engineer. Member AIAA.
‡Professor, Department of Chemical and Materials Engineering. Member AIAA.
§Researcher, CFD Branch. Member AIAA.

incompressible to high-speed compressible flows. The flow-process modeling is further complicated by surface tension, interfacial heat and mass transfer, material property variation, spray formation and turbulence, and their interactions. It is the aim of this study that a general and robust design analysis tool will be available as a result of the incorporation of advanced numerical and physical models in a computational fluid dynamics (CFD) flow solver, the FDNS code.[1,2]

Developments of numerical methods for multiphase free-surface flows were primarily aimed at incompressible flows utilizing the volume of fluid (VOF) method.[3,4] Extensions of the VOF method for atomization simulations have been attempted.[5,6] In Ref. 6 the VOF method was implemented in the ALE–ICE (arbitrary Lagrangian Eulerian–implicit continuous-fluid Eulerian method) algorithm for injector flow simulation with atomization. Because of the inefficiency of the ALE–ICE method, the ARICC-3D was found very time-consuming for multielement computations. Recently, the ALE–ICE method was abandoned by the code developer in favor of the pressure-based SIMPLE algorithm.[7] An alternative approach is to use an embedded grid to fit the liquid-gas interface.[8] A separate parabolic equation of the liquid jet core was derived and solved using a space-marching numerical method. Although this jet-embedding technique offers savings in computational resources, it is not general for various types of atomization processes including impinging jet atomization.

Recently, a combined VOF/Lagrangian multiphase numerical method for all-speed flows was developed.[9] The gas–liquid interface mass, momentum, and energy conservation properties are modeled by continuum surface force (CSF) mechanisms.[10] The CSF method is adopted for its generality and computational efficiency, particularly for three-dimensional computations. The main feature of the present method is to combine the novel feature of the VOF method and the Eulerian/Lagrangian method used in a pressure-based particulate two-phase flow solver[1,2,11] into an algorithm for efficient noniterative, transient calculations of multiphase free-surface flows involving dispersed droplet phases. The present method reformulates the VOF equation to strongly couple two distinct phases (liquid and gas), and tracks droplets on a Lagrangian frame when a spray model is required, using a predictor–corrector technique to account for the nonlinear linkages through the convective contributions of VOF. Formations of droplets and tracking of droplet dynamics are handled through the same unified predictor–corrector procedure. Thus, the new algorithm is noniterative and is flexible in the handling of any general geometries with arbitrarily complex topology in free surfaces. The present method can be applied for transient and steady-state computations and can be implemented into any pressure-based solution method.

Numerical Models

In this approach, a fixed Eulerian mesh system is used to resolve the sharp liquid-gas interface by the concept of a fractional VOF.[9] The present formulation is based on compressible flow governing equations. The forms of the equations are then continuously reduced to their incompressible forms according to the local flow conditions and the VOF solutions. This is the uniqueness of the present method. To illustrate this, the density-weighted averaged conservation equation of mass, Navier–Stokes, and scalar variables in an Eulerian frame work can be written as

$$\frac{\partial \rho_m}{\partial t} + \frac{\partial \rho_m u_j}{\partial x_j} = S_m$$

$$\frac{\partial \rho_m u_i}{\partial t} + \frac{\partial \rho_m u_j u_i}{\partial x_j} = -\frac{\partial p}{\partial x_i} - \frac{\partial}{\partial x_j}\left(\rho_m \overline{u_i' u_j'}\right) + S_u \qquad (1)$$

$$\frac{\partial \rho_m \phi}{\partial t} + \frac{\partial \rho_m u_j \phi}{\partial x_j} = -\frac{\partial}{\partial x_j}\left(\rho_m \overline{u_j' \phi'}\right) + S_\phi$$

The VOF transport equation is given next

$$\frac{\partial \alpha}{\partial t} + u_i \frac{\partial \alpha}{\partial x_i} = S_\alpha \qquad (2)$$

where $\alpha = 1$ stands for liquid and $\alpha = 0$ is for gas. The interface is located at $1 > \alpha > 0$. S_α represents the volume transfer rate across the two-phase boundaries. $\rho_m = (1 - \alpha)\rho_g + \alpha\rho_l$, where ρ_m denotes the time-mean density of the mixture, ρ_g and ρ_l denote gas and liquid density, respectively, u_i and u_i' are the i component of the density-weighted mean and fluctuating part of the instantaneous velocity, ϕ and ϕ' are the density-weighted mean and fluctuating part of the instantaneous scalar quantities including the species concentrations, turbulence quantities, and the gas mixture enthalpy, p is the mean pressure, and S represents sources terms because of mass transfer, momentum transfer, species production, etc. The mixture density is used in the governing equation to represent the present continuum interface model. For pure-liquid or pure-gas regions, the density would recover liquid density or gas density, respectively, based on the mixture density and the interface definitions. Detailed expressions of the source terms can be found in Refs. 1, 2, 9, and 11. In the present study, the turbulent correlation terms $\overline{u_i' u_j'}$ and $\overline{u_i' \phi'}$ are modeled by the two-equation turbulence closure models.[12] For a given solution of the α field, Eq. (1) can be rewritten in the following form to maintain accurate transient from the gas-phase flowfield to the liquid-phase flowfield through the interface:

$$\frac{\partial \rho_m \phi}{\partial t} + \frac{\partial \rho_m u_i \phi}{\partial x_i} = S_\phi, \quad \alpha < 0.05 \quad \text{for compressible gas}$$

$$\rho_m \frac{\partial \phi}{\partial t} + \rho_m u_i \frac{\partial \phi}{\partial x_i} = S_\phi, \quad \alpha \geq 0.05 \quad \text{for interface and liquid}$$

time-step size must be small enough to solve the VOF equation with large source term. For atomization simulations, source terms in the VOF equation such as the mass stripping rate and the resulting droplet size distribution at the liquid–gas interface have to be specified. For example, empirical correlation of Ref. 13 were used for shear coaxial jet atomization calculations in this study. The Lagrangian method of Ref. 11 then is used to track the droplet dispersion within the gas phase. Extra source terms because of the droplet phase are strongly coupled with the Eulerian flow solver using the same operator splitting method as described in Ref. 9. To provide crisp interfacial resolution that is essential for the success of the present VOF method, all test cases were approximated by a high-order upwind total variation diminishing (TVD) scheme[9] for the convection terms. Detailed methodology development and validation of the method for some benchmark gas–liquid flows are described in Ref. 9. We will present the liquid jet atomization in the following section.

Numerical Results

Laminar Impinging Jets

In this test case, three impinging water jets with different impinging half-angle, i.e., 30, 45, and 60 deg were considered. A grid size of 61 × 41 × 41 was generated to simulate the three-dimensional flowfields. The injection speed was 10 m/s and the flowfields were assumed to be laminar. Entrainment boundary conditions are applied at some distance away from the liquid jet. The calculation, which was a transient approach, was terminated at 200 time steps before sheet breakup could occur. Figure 1 shows the predicted flowfields and liquid surface shapes for the three jets. A thin sheet of liquid was formed after impingement. Figure 2 shows the liquid-sheet thickness distribution function and comparisons with an exact solution given by Ref. 14. In this figure, h is the edge thickness (at

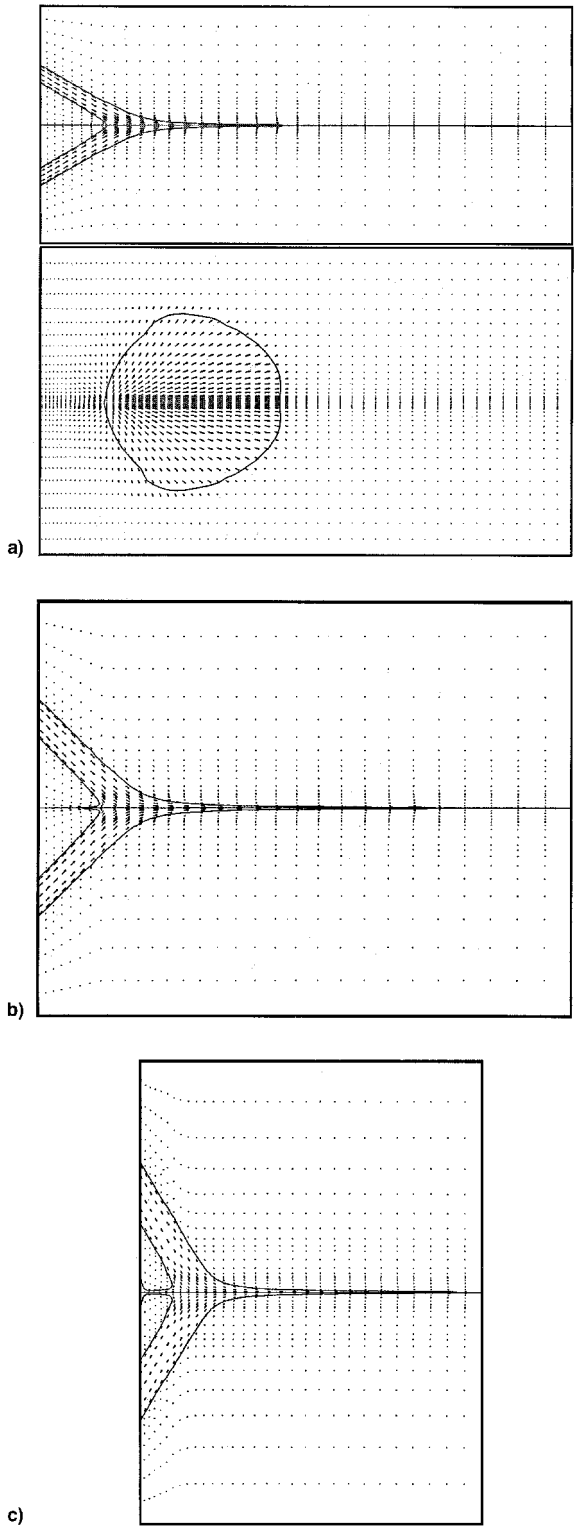

Fig. 1 Laminar impinging jet flowfield. Impinging angle θ: a) 30, b) 45, and c) 60 deg.

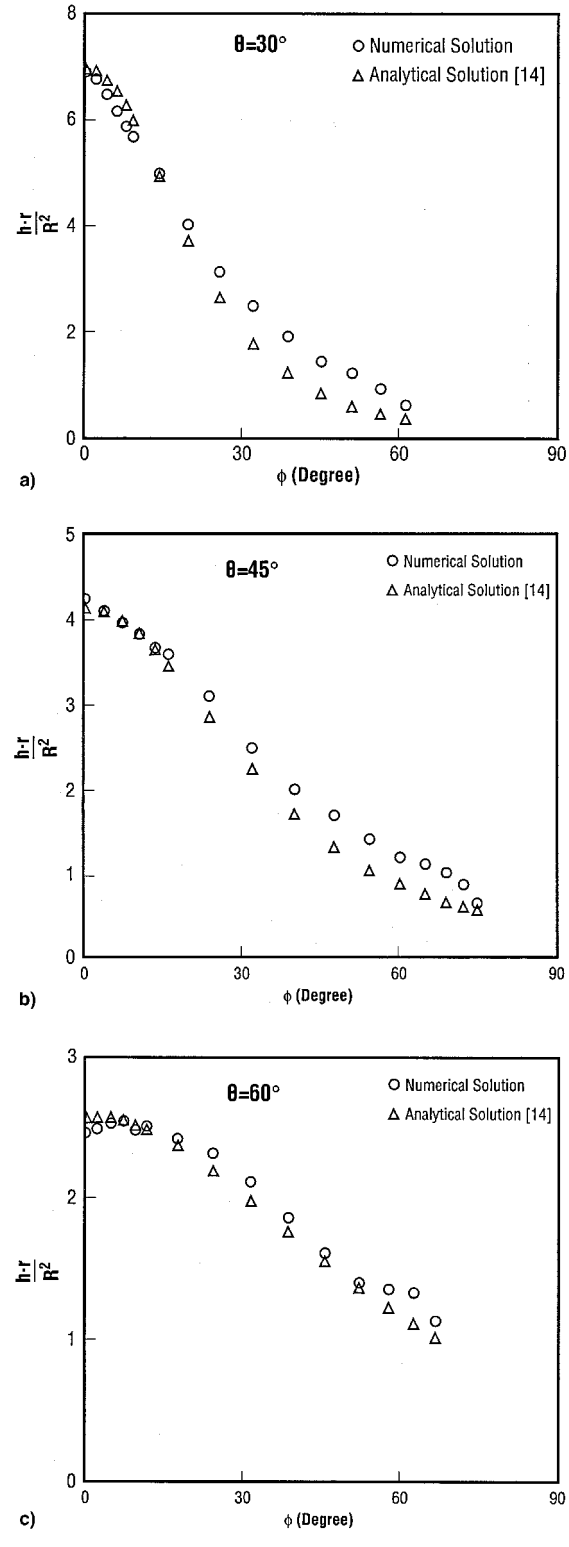

Fig. 2 Variation of sheet edge thickness with angular position and data comparisons. Impinging angle θ: a) 30, b) 45, and c) 60 deg.

radial location r) of the sheet formed by the impinging jets of radius R, and ϕ is the angular position in the sheet formed by the impinging jets.[14] Good agreement is observed from the data comparisons.

Shear Coaxial Liquid Jet Atomization

A cold flow case of coaxial liquid jet atomization reported by Pal et al.[15] was employed to test the current numerical method. Water and gaseous nitrogen were used as the liquid and gas in the study with injection velocity 14.3 and 293 m/s (Mach number around 0.86), respectively. The operating conditions were 300 K and 1 atm. At a distance from the axis, entrainment boundary conditions were applied for the gas phase. A grid size of 61 × 31 was used for the computation. Droplet evaporation effects were included in this calculation, which turned out to have little effect in this case. Figure 3 shows the velocity vectors, liquid core as well as the particle distribution at two different time steps. Liquid jet velocity stays fairly constant because of the large density difference between

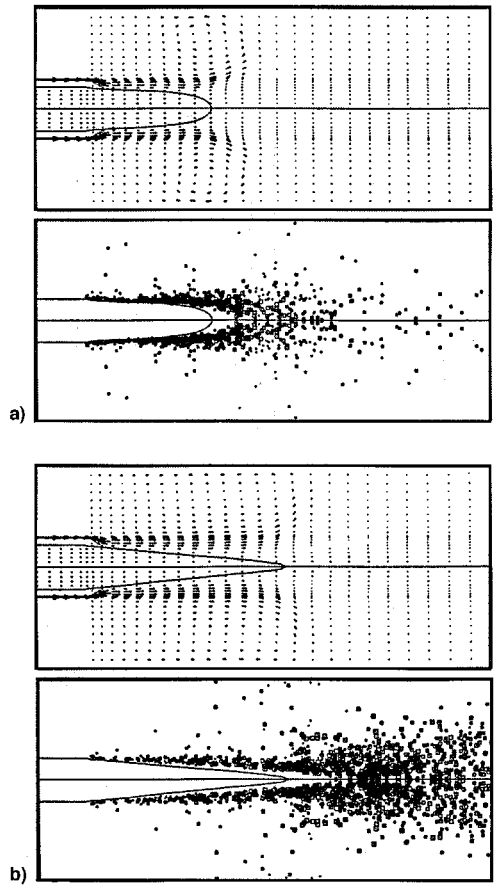

Fig. 3 Velocity vector, liquid core, and droplet trajectories. t = a) 0.6 and b) 1.5 ms.

the two fluids. The numerical model is stable even for large time-step size and for incompressible (liquid)/compressible (gas) flow situation. Particle turbulent dispersion effect[11] has been included and large particle dispersion is shown to be a result of high turbulent intensity of the gas phase. The numerical prediction is reasonable compared to the observed main flow feature.[15]

Summary

This Note summarizes the technical development and validation of a unified multiphase CFD numerical method using the VOF model to analyze general multiphase flow problems involving free surface. A time-accurate multiphase viscous flow solution method has been developed and validated with benchmark test cases including laminar impinging jets and a coaxial jet spray atomization simulation. The gas–liquid interface mass, momentum, and energy conservation properties are modeled by continuum surface force mechanisms. A new solution method is developed such that the present VOF model can be applied for all-speed flow regimes. The main achievements of the present study are the development and incorporation of the fractional VOF cell partitioning approach into a predictor–corrector algorithm to deal with multiphase (gas–liquid) free-surface flow problems; and the coupling of this unified all-speed algorithm with a noniterative Eulerian/Lagrangian particle tracking model. The successful implementation of the VOF model in this study produce a reliable numerical model for spray atomization flow analyses as well as a fundamental building block for a numerical tool which can be used to study complex multiphase flow phenomena that are sometimes hard to visualize experimentally.

References

[1]Wang, T. S., and Chen, Y. S., "Unified Navier-Stokes Flowfield and Performance Analysis of Liquid Rocket Engines," *Journal of Propulsion and Power*, Vol. 9, No. 5, 1993, pp. 678–685.

[2]Chen, Y. S., Liaw, P., Shang, H. M., and Chen, C. P., "Numerical Analysis of Complex Internal and External Viscous Flows with a Second-Order Pressure-Based Method," AIAA Paper 93-2966, 1993.

[3]Torrey, M. D., Cloutman, L. D., Mjolsness, R. C., and Hirt, C. W., "NASA-VOF2D; A Computer Program for Incompressible Flows with Free Surfaces," Los Alamos National Lab., LA-10612-MS, 1985.

[4]Kothe, D. B., and Mjolsness, R. C., "RIPPLE: A New Model for Incompressible Flows with Free Surfaces," *AIAA Journal*, Vol. 30, No. 11, 1992, pp. 2694–2700.

[5]Mayer, W., Labani, R., and Krulle, G., "Theoretical Investigations of Droplet Flow Under Typical Coaxial Injector Flow Conditions in Cryogenic Rocket Engines, AIAA Paper 92-3121, 1992.

[6]Liang, P., and Ungewitter, R., "Multi-phase Simulations of Coaxial Injector Combustion," AIAA Paper 92-0345, 1992.

[7]Liang, P., and Chan, D. C., "Development of a Robust Pressure—Based Numerical Scheme for Spray Combustion Applications," AIAA Paper 93-0902, 1993.

[8]Przekwas, A. J., "Theoretical Modeling of Liquid Jet and Sheet Breakup Processes," *Recent Advances in Spray Combustion: Spray Atomization and Drop Burning Phenomena*, Vol. 1, Progress in Astronautics and Aeronautics, Vol. 166, AIAA, Washington, DC, 1995, pp. 211–239.

[9]Chen, Y. S., Shang, H. M., Liaw, P., Chen, C. P., and Wang, T. S., "A Combined Eulerian-VOF-Lagrangian Method for General Gas-Liquid Flow Applications," *Numerical Heat Transfer*, Vol. 30, Pt. B, 1996, pp. 409–422.

[10]Brackbill, J. U., Kothe, D. B., and Zemach, C., "A Continuum Method for Modeling Surface Tension," *Journal of Computational Physics*, Vol. 100, No. 2, 1992, pp. 335–354.

[11]Chen, C. P., Shang, H. M., and Jiang, "An Efficient Pressure-Velocity Procedure for Gas-Droplet Two-Phase Flow Calculations," *International Journal for Numerical Methods in Fluids*, Vol. 15, No. 2, 1992, pp. 233–245.

[12]Chen, Y. S., and Kim, S. W., "Computation of Turbulent Flows Using an Extended k-ε Turbulence Closure Model," NASA CR-179204, 1987.

[13]Reitz, R. D., "Modeling Atomization Processes in High Pressure Vaporizing Sprays," *Atomization and Spray Technology*, Vol. 3, 1987, pp. 309–337.

[14]Hasson, D., and Peck, R. E., "Thickness Distribution in a Sheet Formed by Impinging Jets," *AIChE Journal*, Vol. 10, No. 5, 1964, pp. 752–754.

[15]Pal, S., Moser, M. D., Ryan, H. M., Foust, M. J., and Santoro, R. J., "Shear Coaxial Injector Atomization Phenomena for Combusting and Non-Combusting Conditions," *Atomization and Spray Technology*, Vol. 6, 1996, pp. 227–244.